Liquid elasticity length, universal dynamic crossovers, and glass transition

2008 J. Phys.: Condens. Matter 20 075103

(http://iopscience.iop.org/0953-8984/20/7/075103)

J. Phys.: Condens. Matter **20** (2008) 075103 (8pp) doi:10.1088/0953-8984/20/7/075103

Liquid elasticity length, universal dynamic crossovers, and glass transition

Kostya Trachenko[1] **and V V Brazhkin**[2]

[1] Department of Earth Sciences, University of Cambridge, Downing Street, Cambridge CB2 3EQ, UK
[2] Institute for High Pressure Physics, RAS, 142190, Troitsk, Moscow Region, Russia

Received 6 November 2007, in final form 6 December 2007
Published 25 January 2008
Online at stacks.iop.org/JPhysCM/20/075103

Abstract

We discuss two main universal dynamic crossovers in a liquid that correspond to relaxation times of 1 ps and 10^{-7}–10^{-6} s. We introduce the concept of liquid elasticity length d_{el}. At room temperature, d_{el} is several Å in water and increases to 0.01 mm in honey and 1 mm in tar. We discuss that on temperature decrease, $d_{el} = d_m$ and $d_{el} = L$ correspond to the two dynamic crossovers, where d_m is the medium-range order and L is system size. In this picture, the two important changes in the dynamics of a system are defined by its fundamental lengths. The second crossover defines all kinetic aspects of the glass transition, whereas the 'thermodynamic' glass transition is realized in the limit of infinite system size only. In this picture, we also discuss the division of liquids into strong and fragile. One prediction of our theory is the increase of viscosity with the size of macroscopic system, which we verify by measuring the viscosity of honey.

1. Introduction

A conceptually simple phenomenon, freezing of liquid into glass, has turned out to be one of the most difficult problems in condensed matter physics, the problem of the glass transition [1, 2]. Analysing the current state of the field, Dyre recently suggested that the glass transition itself is not a big mystery: it universally occurs in any liquid when its relaxation time τ exceeds the time of experiment at the glass transition temperature T_g [2]. The challenges lie above T_g: explaining the physical origin of the most important anomalous relaxation properties of a liquid in the glass transformation range, the Vogel–Fulcher–Tammann (VFT) law and stretched-exponential relaxation [1, 2]. To these, one can add the origin of two universal dynamic crossovers.

If we consider the changes in dynamics in a liquid on lowering the temperature, we find two dynamic crossovers. The first crossover is at high temperature at liquid relaxation time $\tau_1 \approx 1$ ps, at which the dynamics changes from exponential relaxation, $q(t) \propto \exp(-t/\tau)$, to stretched-exponential relaxation, $q(t) \propto \exp(-(t/\tau)^\beta)$, where q is a relaxing quantity and $0 < \beta < 1$. This crossover is universal, i.e. is seen in many systems [3–8]. As the temperature is lowered, we find another universal crossover at $\tau_2 = 10^{-7}$–10^{-6} s [9, 10]. This crossover also marks the qualitative change in the system's dynamics. A notable manifestation of this change is the transition from the VFT law to Arrhenius relaxation. Many other properties have been found to show a crossover at τ_2 as well [9–15]. The second crossover was called the transition from the 'liquid-like' to the 'solid-like' behaviour [10]. Note that although the relaxation time at the second crossover is much larger as compared to the first one, it is still about nine to ten orders of magnitude smaller than the relaxation time at the glass transition ($\approx 10^3$ s).

The physical origin of the two universal dynamic crossovers is not known. Explaining it should form an important part of a theory of the glass transition.

An important general question is what a theory of glass transition should be based on. Previous theories identified different variables which control the process of glass transition, including entropy, volume, energy landscape and many others [2]. Each variable implies a different mechanism of glass transition. We believe that a successful glass transition theory should discuss how the stress relaxation mechanism of a liquid changes on lowering the temperature. This is because a glass is different from a liquid by virtue of its ability to support shear stress; hence, stress relaxation, or elasticity, is the central physical property as far as glass transition is concerned. This requirement for a glass transition theory can now be strengthened by asking a theory to explain the anomalous phenomena of the glass transition on the basis of elastic properties of a liquid only, without invoking additional ideas or mechanisms. This is the view that we adopt and

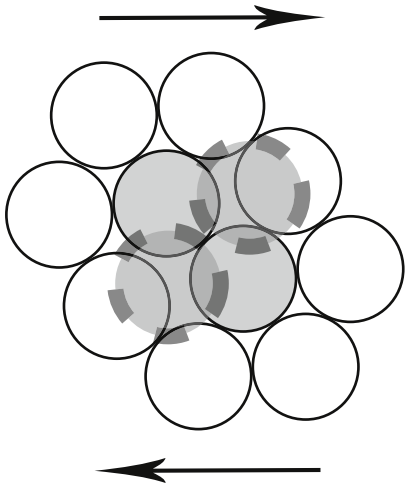

Figure 1. Orowan's example of a concordant local rearrangement [16]. Solid and dashed lines around the shaded atoms correspond to initial and final positions of a rearrangement, respectively. The arrows show the direction of external stress.

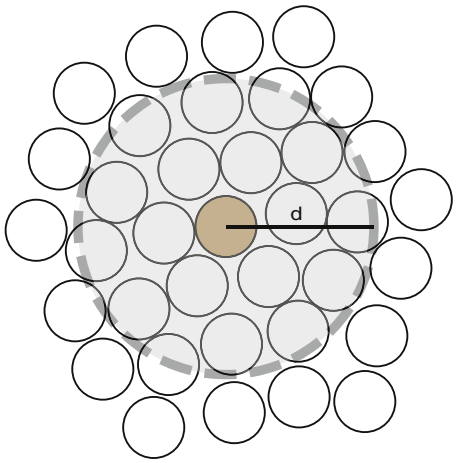

Figure 2. Illustration of the elastic interaction between local relaxation events. This interaction takes place within the range $d_{\rm el}$ from the central relaxing regions. Shaded and open circles represent local relaxing regions inside and outside, respectively, the interaction sphere.

explore in this paper: we seek to understand glass transition solely on the basis of stress relaxation of a liquid.

In order to understand the origin of the two dynamic crossovers, we begin the discussion by studying how stress relaxation of a liquid changes on lowering the temperature. We introduce the temperature-dependent liquid elasticity length, which is the range of elastic interaction in a liquid. Several Ångstroms at high temperature, this length grows with relaxation time of the system, increasing sharply on lowering the temperature. We propose that that the first and second dynamic crossovers take place when this length becomes equal to the values of the medium-range order and system size, respectively. In this picture, we discuss how the second dynamic crossover is related to the old question of whether the glass transition is a thermodynamic or kinetic phenomenon. The division of liquids into strong and fragile is also discussed. Finally, we perform the experimental measurement of viscosity at different values of liquid elasticity length to test the prediction of our theory that viscosity increases with the size of the macroscopic system.

2. Liquid elasticity length

In this section, we introduce the important concept of liquid elasticity length, and discuss how it compares with characteristic lengths in a disordered system. We first note that no characteristic length scale is present in the usual elastic theory of a solid: elastic strains and stresses continuously decay as $\propto 1/r^2$ and $\propto 1/r^3$, respectively. On the other hand, as we discuss below, a dynamically relaxing liquid does have a length scale beyond which elastic interaction does not operate.

Let us consider relaxation in a liquid under, for example, shear stress. Such a relaxation is the sequence of elementary localized structural rearrangements, local relaxation events (LREs). Because the divergence of the elastic field due to an LRE is zero, an LRE is not accompanied by density changes of the surrounding liquid, and can be viewed, in a simple model, as a pure shear event [2]. For the purpose of discussing the interaction between LREs through their elastic fields, we can therefore ignore the longitudinal component of the elastic field due to an LRE and consider shear events. A typical shear relaxation event is shown in figure 1 (the term 'concordant' in the figure caption is not important here, and will be explained in the next section).

A structural rearrangement, that accompanies an LRE, produces elastic shear stress that can propagate through the system. The important question is how this stress affects the relaxation of other LREs in the system.

Let us consider how LREs interact elastically in some detail, and discuss how the changes of stresses due to remote shear LREs affect a given local relaxing region, shown in the centre in figure 2. Relaxation of the central event involves deformation of the 'cage' around the jumping atom (see figure 1), and therefore depends on the stresses that propagate from the remote LREs to the centre. A remote shear LRE, similar to the one shown in figure 1, creates elastic shear waves of different frequencies. Among these frequencies, high-frequency waves are present, because the deformation associated with an LRE creates a wave with a length comparable to the interatomic separation (see figure 1), and hence with a frequency on the order of the Debye frequency. At high frequency, larger than the inverse of τ, a liquid can support shear stress just like a solid. Hence the high-frequency shear waves from all remote LREs propagate the stress and its variations to the central point. However, not all of these affect the relaxation of the central LRE, but only those that are located within the distance $d_{\rm el} = c\tau$ from the centre, where c is the speed of sound. This is because the stresses that arrive at the centre from larger distances take a time longer than τ to travel, during which a local event in the centre already relaxes (the time between consecutive LREs is given by τ). After time τ a new LRE happens in its place or nearby, and the process repeats.

$d_{\rm el}$, therefore, captures the dynamic process of relaxation in a liquid, and defines the maximal distance at which two shear

Table 1. Approximate values of viscosity η, relaxation time τ and liquid elasticity length d_{el} at room temperature.

Liquid	η (Pa s)	τ (s)	d_{el}
Water, olive oil, Ethanol, glycerol	10^{-3}–1	10^{-13}–10^{-11}	1–1000 Å
Honey	10–10^{2}	10^{-9}–10^{-8}	1–10 μm
Tar	10^{4}	10^{-6}	1 mm
Pitch	10^{8}	10^{-2}	10 m

LREs elastically interact. For this reason, we call it the *liquid elasticity length*.

Because c is on the order of a/τ_0, where a is the interatomic separation of about 1 Å and τ_0 the oscillation period, or the inverse of the Debye frequency ($\tau_0 = 0.1$ ps), we find

$$d_{el} = c\tau = \frac{\tau}{\tau_0}a. \quad (1)$$

To illustrate the actual values of the introduced elasticity length in real liquids at room temperature, we have calculated d_{el} from equation (1) using the experimental values of viscosity η and Maxwell relation $\eta = \tau G_\infty$, assuming $G_\infty \approx 10$ GPa and $c \approx 1000$ m s^{-1}. The results are summarized in table 1. Starting from 1–1000 Å in familiar liquids like water or olive oil, d_{el} increases to 0.01 mm in honey and to 1 mm in very viscous tar. In extremely viscous pitch, $d_{el} = 10$ m. An interesting observation here is that for most familiar liquids, d_{el} does not exceed their typical experimental sizes. The subject of system size will be discussed in this section as well as throughout this paper.

If V is the activation barrier for an LRE (V can be temperature dependent), $\tau = \tau_0 \exp(V/kT)$, and increases on lowering the temperature. According to equation (1), this results in an increase of the range in which LREs elastically interact.

Our main proposal in this paper is that the key to the dynamic crossovers is the increase of d_{el} on lowering the temperature, when d_{el} crosses two characteristic lengths in a liquid. Recall that in a perfect crystal there are two fundamental lengths, lattice constant a and system size L. In a disordered system like a liquid, there is an additional length d_m, which corresponds to the medium-range order, and is defined by local packing. d_m is on the order of 10 Å, the characteristic size of decay of structural correlations in a disordered medium. d_m can weakly depend on the substance and external parameters (temperature, pressure).

On lowering the temperature, d_{el} crosses all three fundamental lengths in a system. At high temperature, d_{el} is on the order of interatomic distance a (see equation (1)). On lowering the temperature, τ increases as $\tau = \tau_0 \exp(V/kT)$, and d_{el} quickly increases to d_m. Because d_m is on the order of 10 Å, we find from equation (1) that $d_{el} = d_m$ gives τ of about 1 ps. This is the first dynamic crossover discussed above. On lowering the temperature even further, equation (1) shows that d_{el} increases to L. In liquid relaxation experiments, L is typically 1–10 mm (see the discussion below). According to equation (1), $d_{el} = L$ gives $\tau = 10^{-7}$–10^{-6} s, the second dynamic crossover. The two crossovers are illustrated in figure 3.

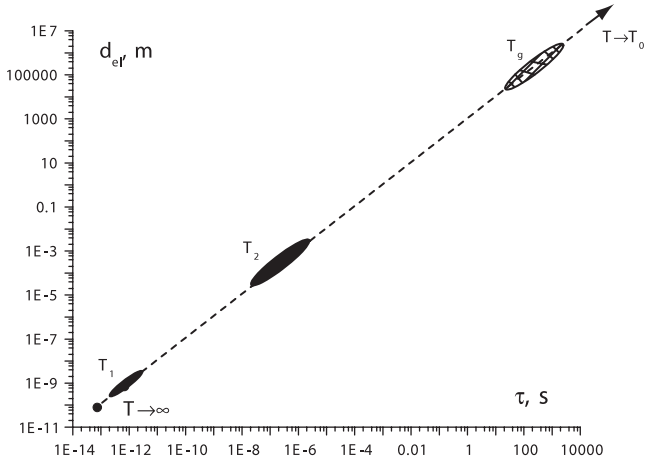

Figure 3. Elasticity length d_{el} as a function of relaxation time. T_1 and T_2 correspond to two dynamic crossovers. T_g and T_0 are glass transition and VFT temperatures, respectively.

We propose that the physical reason for the two dynamic crossovers is related to the two qualitative changes of the relaxation mechanism in a liquid on lowering the temperature when d_{el} reaches d_m and L. A typical distance between the neighbouring LREs is about 10 Å, or d_m. At high temperature, when $d_{el} < d_m$, the elastic interaction between LREs is absent, and LREs take place independently. When $d_{el} = d_m$, LREs start elastically interact, resulting in the *first* dynamic crossover, which corresponds to the crossover from independent to non-independent relaxation. On lowering the temperature, d_{el} increases. In the temperature range which gives $d_m < d_{el} < L$, relaxation takes place in partially 'elastic' liquid, i.e. LREs elastically interact, but only in the range given by d_{el}. Finally, when, on lowering the temperature, $d_{el} = L$, all LREs in a system start interacting with each other. This corresponds to the transition from partially elastic to wholly elastic liquid, and gives the *second* dynamic crossover. This process will be discussed below in more detail.

Hence, d_{el}, introduced in this section, plays the central role in our discussion. In the next section we introduce the elastic feed-forward interaction mechanism between LREs. The physical importance of d_{el} is that it sets the range of this interaction.

3. Elastic feed-forward interaction mechanism

Some time ago, Orowan introduced 'concordant' local rearrangement events to discuss creep phenomena [16]. A concordant local rearrangement is accompanied by a strain agreeing in direction with the applied external stress, and reduces the energy and local stress (see figure 1). A discordant rearrangement, on the other hand, increases the energy and local stress. This has led to a general result that stress relaxation by earlier concordant events leads to the increase of stress on later relaxing regions in a system. Goldstein applied the same argument to a viscous liquid [17]: consider a system under external stress which is counterbalanced by stresses

supported by local regions. When a local rearrangement to a potential minimum, biased by the external stress, occurs (a concordant event), this local region supports less stress after the event than before; therefore, other local regions in the system should support more stress after this event than before [17].

Let us consider relaxation in a liquid induced by an increment of external shear stress. As argued by Orowan and Goldstein, because an external shear stress introduces bias towards concordant shear relaxation events, which support less shear stress after relaxation, later relaxing regions should support more shear stress in order to counterbalance the decrease. If Δp is the corresponding increase of stress on a currently relaxing region and n is the current number of LREs, Δp is a monotonically increasing function of n.

The increase of stress, Δp, on a currently relaxing region increases its activation barrier V. It has been argued that V is given by the elastic shear energy of a surrounding liquid [2, 18–20]. As discussed by Dyre *et al* [20], the energy needed for an atom to escape its cage at the constant volume is very large because of the strong short-range interatomic repulsions, hence it is more energetically favourable for the cage to expand, reducing the energy needed for escape. Such an expansion results in the elastic deformation of the surrounding liquid, hence the activation barrier is given by the work of the elastic force needed to deform the liquid around an LRE [20]. Because such a deformation does not result in the volume change of the surrounding liquid (for the displacement field $\mathbf{u}$ created by the expanding sphere, $\mathrm{div}(\mathbf{u}) = 0$), it has been argued that V is given by the shear energy of the surrounding liquid [20]. This result was confirmed by the experimental data, showing that the activation barrier increases with the shear energy [20].

Because, as discussed by Orowan and Goldstein, previous LREs reduce stress in the direction 'concordant' to the external stress (see figure 1), the increase of shear stress on later rearranging regions consistently increases shear strain on them in the same direction, increasing shear energy and therefore V. The increase of V due to the additional stress Δp, ΔV, is given by work $\int \Delta p \, \mathrm{d}q$. If q_a is the characteristic activation volume [20], $\Delta V = \Delta p q_\mathrm{a}$, and we find $V = V_0 + q_\mathrm{a}\Delta p$, where V_0 is the high-temperature activation barrier.

Because Δp is a monotonically increasing function of n and $V = V_0 + q_\mathrm{a}\Delta p$, we find that V is also a monotonically increasing function of n. This provides the *elastic feed-forward interaction mechanism* between LREs [21], in that activation barriers increase for later events. As discussed in the previous section, the range in which this elastic interaction mechanism operates is given by d_el.

We have recently shown that the two most important signatures of the glass transformation range, stretched-exponential relaxation and the VFT law, can be derived on the basis of the feed-forward interaction. For details of calculation the reader is referred to [21, 22]. Below we discuss how the elastic feed-forward interaction mechanism gives rise to the two dynamic crossovers on lowering the temperature when $d_\mathrm{el} = d_\mathrm{m}$ and $d_\mathrm{el} = L$.

4. Comment on cooperativity of relaxation

It is interesting to note the relationship between the elastic interaction mechanism discussed in the last two sections and 'cooperativity' of molecular motion. Cooperativity, which is absent at high temperature, but becomes operative in a liquid at low temperature, has been discussed intensely in the area of glass transition [2, 23, 24]. For example, the entropy theory, as well as other approaches to the glass transition, assume the existence of 'cooperatively rearranging regions', 'domains' or 'clusters' in a liquid (for review, see [23]), in which atoms move in some concerted way that distinguishes these regions from their surroundings. On lowering the temperature, the size of this region can grow, but does not exceed several nanometres [23]. The physical origin of this cooperativity has not been understood, nor has the nature of the concerted motion, and remains one of the central open questions in the field of glass transition [2, 23, 24].

Here, we do not need to assume the existence of cooperativity of relaxation as in the previous work [2, 23, 24]. In our discussion, the elastic interaction between LREs is the necessary feature of relaxation that becomes operative in a liquid on lowering the temperature: as discussed above, this interaction is absent when $d_\mathrm{el} < d_\mathrm{m}$, but becomes operative when $d_\mathrm{el} > d_\mathrm{m}$. Hence, in our picture, relaxation is 'cooperative' in a general sense that LREs are not independent, but the origin of this cooperativity is the usual elastic interaction. Consequently, instead of the size of a cooperatively rearranging region discussed previously [2, 23], we operate in terms of the range over which interactions are elastic in a liquid. The important quantitative difference between the size of a cooperatively rearranging region and our elasticity length d_el is that the former does not exceed several nanometres [23], whereas the latter becomes macroscopic above T_g: if $\tau(T_\mathrm{g}) = 10^3$ s, $d_\mathrm{el} = 1000$ km at T_g, according to equation (1).

5. The first dynamic crossover

The elastic interaction between LREs, discussed in the previous sections, sets the stage for clarifying the origin of the two dynamic crossovers.

Because, as discussed above, $d_\mathrm{el} < d_\mathrm{m}$ at high temperature, the elastic feed-forward interaction is absent, and LREs do not interact. When LREs are independent, it is easy to derive the expected high-temperature result that relaxation is Debye (exponential) in time [21]. On the other hand, when $d_\mathrm{el} \geqslant d_\mathrm{m}$ on lowering the temperature, the elastic feed-forward interaction between LREs becomes operative. We have recently shown that stretched-exponential relaxation follows as a result [21]. Hence $d_\mathrm{el} = d_\mathrm{m}$ marks the crossover from exponential to stretched-exponential relaxation.

According to equation (1), $d_\mathrm{el} = d_\mathrm{m}$ gives

$$\tau_1 = \frac{d_\mathrm{m}}{a}\tau_0. \tag{2}$$

Because $\tau_0 = 0.1$ ps and d_m/a are roughly system and temperature independent, equation (2) predicts that τ_1 is a universal parameter. This is consistent with experimental

findings [3–8]. Because d_m/a is on the order of 10, we find from equation (2) that τ_1 is about 1 ps, in good agreement with the experimental value in the 1–2 ps range [3–8].

6. The second dynamic crossover

To discuss the second dynamic crossover, we first discuss how V changes with d_{el}. To calculate V as a function of d_{el}, let us consider relaxation induced by an increment of external shear stress. It involves a finite number of LREs, and we consider, for simplicity, the last LRE to relax to be in the centre of the sphere of radius d_{el} (see figure 2). The stress on the central rearranging region increases in order to counterbalance the decreases of stresses due to the previous remote concordant LREs. These LREs are located within the range of the feed-forward interaction d_{el} (see figure 2). It is easy to see that the increase of stress, Δp, on the central region increases with d_{el}: as d_{el} increases, this region needs to counterbalance the reductions of stresses due to an increasing number of remote concordant LREs. Δp can be explicitly calculated as a function of d_{el}. Joining the result with $V = V_0 + q_a \Delta p$ from section 3 gives [21, 22]

$$V = V_0 + C \ln\left(\frac{2d_{el}}{d_0}\right) \tag{3}$$

where d_0 is the size of a local rearranging region and C depends on microscopic parameters of the system.

We note here that in equation (3) V implicitly depends on temperature through d_{el}. Using $\tau = \tau_0 \exp(V/kT)$ in equation (1) and combining it with equation (3) gives the explicit temperature dependence of V. As we have recently shown, this gives the VFT law for the activation barrier $V = AT/(T - T_0)$ and relaxation time $\tau = \tau_0 \exp(A/(T - T_0))$ [22]. Here, the super-Arrhenius behaviour is related to the increase of the range of the feed-forward interaction, d_{el}: as the temperature is lowered, more LREs are involved in the elastic interaction with a currently relaxing event, increasing its activation barrier.

We are now ready to discuss the second dynamic crossover. According to equation (3), V increases with d_{el} on lowering the temperature as long as $d_{el} < L$. When $d_{el} = L$, all LREs in the system are involved in the feed-forward interaction. Hence $d_{el} = L$ marks the transition of the system from being partially to wholly 'elastic', and should manifest itself as a qualitative change in the liquid's dynamics. The important aspect of such a change directly follows from equation (3): at $d_{el} > L$, $V \propto \ln(L)$, and is temperature independent. To be more precise, when $d_{el} > L$, further decrease of temperature has a weaker effect on V, related to, e.g., density increase, but not to the increase of d_{el}. As a result, the system is expected to show a crossover to a more Arrhenius behaviour. This will be discussed in more detail below.

Setting $d_{el} = L$ gives, according to equation (1),

$$\tau_2 = \frac{L}{a}\tau_0. \tag{4}$$

Equation (3) predicts that, similar to τ_1, τ_2 is a universal parameter, independent of temperature or system type. This is consistent with experimental findings [9, 10, 12–15]. Typical values of L used in the experiments are 1–10 mm, which is dictated mostly by the experimental set-up. For example, smaller system sizes can be associated with surface effects, while larger system sizes can involve temperature gradients and effects of final thermal conductivity. Furthermore, fragile systems of larger size can not be supercooled without crystallization. Using the range of L = 1–10 mm and τ_0 = 0.1 ps, we find from equation (4) that $\tau_2 = 10^{-7}$–10^{-6} s. This is in good agreement with experimental results, which show that for many studied materials $\tau_2 = 10^{-7}$–10^{-6} s, although exceptions have been noted [15]. Note that at the second $d_{el} = L$ crossover $1/\tau_2$ has the meaning of the typical values of eigenfrequencies of the system.

Experimentally, there is ample evidence for the second dynamic crossover in many systems. Most direct evidence comes from the sharp kink in the dielectric function [9]. The crossover to the lower slope of relaxation time, with the effect that the glass transition becomes retarded, is observed [11], in agreement with the prediction from our picture. Other experiments include NMR relaxation data, which detect a similar dynamic crossover [12], the crossover in the relaxation of cage sizes in the positron annihilation experiments [13] and changes of non-ergodicity parameter [14].

It is interesting to ask what kind of room temperature liquid has viscosity that corresponds to the second dynamic crossover $\tau_2 = 10^{-7}$–10^{-6} s. From table 1, we observe that τ_2 corresponds to a viscosity of 10^3–10^4 Pa s. This is much larger than the room temperature viscosity of familiar liquids like water, ethanol, or olive oil, for which η is in the 10^{-3}–1 Pa s range, or honey (η = 10–10^2 Pa s). These examples show that although the second crossover is long above the glass transition, it corresponds to quite high values of viscosity. From table 1 we find that very viscous tar ($\eta = 10^4$ Pa s) has relaxation time close to τ_2 and d_{el} = 1 mm, comparable with typical experimental system sizes. This illustrates that the second dynamic crossover $d_{el} = L$ corresponds to a very viscous medium like tar.

From the physical point of view, the results of this as well as the previous section are interesting, in that we have shown that there is a simple relationship between structure and dynamics: the most important changes in the dynamics of a disordered system are defined by its fundamental lengths only (see equations (2) and (4)). This is a new general result, not discussed before.

7. Is the glass transition a thermodynamic or kinetic phenomenon?

In this section, we discuss how the second dynamic crossover at $d_{el} = L$ is related to the old debate about whether the glass transition should be viewed as a thermodynamic or kinetic phenomenon. As discussed in the previous section, the increase of d_{el} on lowering the temperature gives the VFT law for relaxation time, $\tau = \tau_0 \exp(A/(T - T_0))$ [22]. Because τ formally diverges at T_0, several models have suggested that an underlying phase transition can exist. However, the nature of this transition and the second phase is not clear. This, together

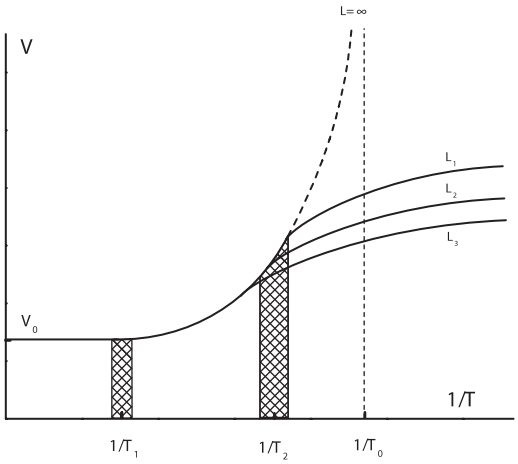

Figure 4. The effect of the elastic feed-forward interaction on the activation barrier V. V increases from its high-temperature value at the first dynamic crossover at temperature T_1 to the second dynamic crossover at T_2. After the second crossover at $d_{el} = L$, V starts saturating to a constant value depending on the system size L: the larger L, the larger value of V can be achieved. For finite system size, the divergence of relaxation time takes place at zero temperature only. For the infinite system, V grows to infinity, resulting in the divergence at the finite VFT temperature T_0.

with the fact that no phase transition is seen when a liquid forms a glass, continues to fuel the current debate [1, 2].

In our discussion, the debate related to the nature of the glass transition is settled as follows. Because, according to equation (1), $d_{el} \propto \tau$, we find that $d_{el} \propto \exp(A/(T - T_0))$. When T approaches T_0, d_{el} diverges, and exceeds any finite size of the system L. When $d \geqslant L$, all events in the system participate in the elastic feed-forward interaction mechanism, and there is no room for the increase of V by way of increasing d_{el}. As a result, relaxation stops following the VFT dependence, and tends to Arrhenius, pushing the divergence to zero temperature. We therefore find that only the truly infinite system $L = \infty$ does not have the second dynamic crossover, and has the divergence of relaxation time at the finite VFT temperature T_0. This is illustrated in figure 4.

We note that in this picture, no dynamic crossover takes place at T_g, consistent with the experimental observations. According to equation (1), $T_g = 10^3$ s corresponds to d_{el} of 1000 km, which explains why the two dynamic crossovers are seen long before T_g is reached (see figure 3). In other words, the absence of a dynamic crossover in the vicinity of T_g is due to the imbalance between our typical experimental times and sample sizes: at typical experimental time, the elasticity length is more than eight orders of magnitude larger than the typical experimental length. In this context, we note that the temperature and magnitude of the anomalies of thermodynamic properties seen at T_g are sensitive to cooling rates and observation times. Were the thermodynamic parameters measured at higher cooling rates and shorter experimental times, they would show the anomalies at temperatures that correspond to relaxation time τ_2. We also note that the thermodynamic anomalies seen at T_g have real thermodynamic meaning only at T_0, which, as discussed above, can be reached only for the infinite system.

It therefore follows from our discussion that liquids on cooling present a unique case when the thermodynamic limit for the phase transition is not reached for any macroscopic size of the system. Furthermore, system size itself defines the temperature and existence of the second crossover from a 'liquid-like' to 'solid-like' behaviour. In this sense, solidification of a liquid is dramatically different from behaviour in crystals, where the thermodynamic limit, for practical purposes, is reached for a sufficiently large (10^6) number of atoms, whereas finite size effects come into place at the nanoscale only.

Therefore we conclude that d_{el} plays the role of the order parameter for the glass transition, albeit with unusual properties: in a finite system, $d_{el} = L$ marks the dynamic crossover without a true thermodynamic transition, whereas $d_{el} = L$ corresponds to a true thermodynamic transition in the infinite 'thermodynamic' liquid (see figure 4).

8. Comment on liquid's fragility

Experimentally, various liquids show different curvatures of $\ln(\tau)$ as a function of T_g/T, or different degrees of deviation from the Arrhenius relaxation $\ln(\tau) \propto 1/T$ [25]. This diversity can be modelled by different parameters A and T_0 in the VFT equation. The degree of deviation from the Arrhenius law was proposed to be called liquid 'fragility', the larger the deviation, the larger the fragility [26]. Liquids with small and large deviations from the Arrhenius law were further proposed to be called 'strong' and 'fragile', respectively. The physical origin of fragility has remained an open problem since, adding to controversy in the field [2].

The physical origin of fragility must be related to the origin of the VFT law: if a certain process is responsible for the deviation from the Arrhenius relaxation in the form of the VFT law, the strength of this process sets fragility. In our picture, the origin of the VFT law is the increase of d_{el} on lowering the temperature. The origin of fragility can similarly discussed in this approach. According to equation (3), as long as at high temperature $d_{el} < L$, lowering the temperature increases V, resulting in a fragile behaviour. If, on the other hand, $d \geqslant L$ at high temperature already, further decrease of temperature has a weaker effect on V, giving weak super-Arrhenius behaviour. Experimentally, for many systems the studied range of temperatures varies from about $2T_g$ and T_g [8], hence we consider the increase of d_{el} from high temperature $T_h = 2T_g$ to T_g. Take, for example, two systems on the stronger side of fragility plots, BeF_2 and SiO_2. From the experimental values of V_h/kT_g (V_h is the activation barrier at the highest measured temperature), we find $V_h/kT_h = 24$ and 19.6 for BeF_2 and SiO_2, respectively [27]. Using $\tau = \tau_0 \exp(V/kT)$ in equation (1), we find $d_{el} = a \exp(V/kT)$, giving $d_{el} = 2.6$ m and 33 mm at T_h for the two systems. As discussed above, typical values of L used in the experiments are 1–10 mm, hence our picture correctly predicts that these systems should be on the strong end of fragility plots. For two fragile systems, toluene and propylene carbonate, $V_h/kT_h = 3.34$ and 5.75, respectively, giving d_{el} of 28 and 314 Å, respectively. This is much smaller than L, hence our picture predicts that these systems should be fragile, as is seen experimentally.

In this picture, strong systems should have large intrinsic (i.e. unrelated to the increase of d_{el}) activation barriers, so that $d_{el} \geqslant L$ already at high temperature. For example, covalent liquids have the large activation energy needed to break strong covalent bonds, and are therefore expected to be on the stronger end of fragility plots. Fragile systems, on the other hand, should have smaller intrinsic activation barriers, so that $d_{el} \ll L$ at high temperature. This is characteristic of, for example, ionic liquids, in which local rearrangement processes are not accompanied by the change of electronic structure to the same extent as in covalent liquids, and hence cost less energy. This picture therefore predicts covalent and ionic liquids to be generally on the strong and fragile ends of fragility plots, respectively, consistent with experiments [26]. There may be other factors that define intrinsic activation barriers. Regardless of these, however, the physical origin of fragility in our picture is the increase of d_{el} on lowering the temperature.

One interesting prediction from this picture is that liquids which appear to be strong on the fragility plots (e.g. SiO_2, GeO_2) can show signs of increased fragility when the measurements are extended to higher temperature so that d_{el} decreases below L (for some of the strong systems, high-temperature data are absent in fragility plots [26], which is probably related to measurement difficulties at high temperatures). In this picture, all liquids should show deviations from purely Arrhenius relaxation if the temperature range is large enough to include the case $d_{el} \ll L$.

In this sense, the difference between strong and fragile liquids is not qualitative, or fundamental, from the physical point of view. Rather, the difference is quantitative, in that depending on the relative weight of the first and second term in equation (3) a liquid can show a larger or a smaller deviation from the Arrhenius behaviour in the temperature range where $d_{el} < L$.

It should be noted that the increase of V due to the increase of d_{el} is not the only possible mechanism of super-Arrhenius behaviour and fragility. For example, in some systems V can noticeably increase due to density increase on lowering the temperature. The corresponding contribution to the increase of V depends on temperature dependence of density. Note that whereas system size does not affect the density-related increase of V it affects the increase of V due to the increase of d_{el}. In the next section, we discuss this effect in more detail.

9. Experimental results for the system size effect

The discussed picture of the glass transition makes a specific prediction regarding the effect of system size on viscosity. It follows from the above discussion that V, and hence apparent viscosity, is not a local property, but is governed by the elastic interaction between local regions within range d_{el}. When d_{el} crosses system size at low temperature, viscosity is defined by interactions between all local regions in the system. According to equation (3), V and η are independent of system size for $d_{el} < L$, but increase with L when $d_{el} \geqslant L$. Hence an unusual prediction, the increase of viscosity with system size, emerges from this picture. Below we test this prediction experimentally.

Table 2. Viscosities η_1 and η_2 measured in containers of length $L_1 = 10$ mm and $L_2 = 50$ mm. The calculated values of d_{el} at five temperatures are also shown.

T (K)	d_{el} (mm)	η_1 (Pa s)	η_2 (Pa s)
306	0.003	8.1 ± 0.5	8.2 ± 0.5
293	0.01	26 ± 2	25.5 ± 2
279	0.08	210 ± 15	215 ± 15
254	45	$(0.9 \pm 0.1) \times 10^5$	$(1.2 \pm 0.1) \times 10^5$
248	110	$(2.1 \pm 0.2) \times 10^5$	$(2.9 \pm 0.2) \times 10^5$

We have chosen honey as an appropriate liquid for our experiment since its elasticity length crosses system sizes in a convenient temperature range (see below). We have measured viscosity by measuring the falling time of a steel ball using the Stokes equation with the end and wall correction, $\eta = 2gr_b^2(\rho_b - \rho_l)W/9vE$, where $W = 1 - 2.104(r_b/r_c) + 2.09(r_b/r_c)^3 - 0.95(r_b/r_c)^5$ and $E = 1 + 3.3(r_b/h)$. Here, v is the measured falling velocity, g is the acceleration due to gravity, ρ_b and ρ_l are the densities of the ball (7.7 g cm^{-3}) and the liquid (1.45 g cm^{-3}), r_b and r_c are the radii of the ball ($2r_b = 1.55$ mm) and container, respectively, and h is the container height taken to be the falling distance. We have measured η at 306, 293, 279, 254, and 248 K in two different containers, of $L_1 = 10$ mm in diameter and $L_1 = 10$ mm in height, and $L_2 = 50$ mm in diameter and $L_2 = 50$ mm in height. The corresponding values of η_1 and η_2 are shown in table 2. Also shown are the values of d_{el} calculated from equation (1), where τ is calculated from the Maxwell relation $\eta = \tau G_\infty$, $G_\infty \approx 4$ GPa.

Consistent with the theoretical prediction, we find that for $d_{el} < L$, $\eta_1 = \eta_2$. On the other hand, for $d_{el} \geqslant L$, we observe that $\eta_1 < \eta_2$: for $d_{el} = 110$ mm, the viscosity is about 40% larger in the larger container as compared to the smaller one. The observed increase of viscosity with system size is an interesting unexpected effect. It would certainly be interesting to study it in other systems. Since no other theory predicts that viscosity should increase with system size, we believe that this specific result lends good support to the elastic picture of glass transition that we discussed.

We conclude this section by noting that the increase of V can have a contribution related to the increase of density. This contribution comes in addition to the increase of d_{el}, and does not depend on system size. Hence the effect of system size on viscosity can be reduced depending on the relative weight of two contributions that arise from the increase of d_{el} and density.

10. Summary

In summary, we have introduced the concept of liquid elasticity length d_{el}, and discussed that when d_{el} becomes equal to the medium-range length and system size on lowering the temperature two universal dynamic crossovers take place. From a physical point of view, an interesting conclusion that follows is that the most important changes in the dynamics of a disordered system are defined by its fundamental lengths only. The discussion of the second dynamic crossover is directly related to the old debate between the proponents of 'kinetic'

and 'thermodynamic' views of the glass transition, and we have discussed that the glass transition is a kinetic process for any finite system, and is a thermodynamic transition for the infinite system. Finally, we have experimentally tested the prediction of our theory that apparent viscosity increases with the size of a macroscopic system.

Acknowledgments

We are grateful to R Casalini, M Roland, and M T Dove for discussions, and to EPSRC for support.

References

[1] Langer J 2007 *Phys. Today* **60** (February) 8
[2] Dyre J C and Dyre J C 2006 *Rev. Mod. Phys.* **78** 953
[3] Roland C M, Ngai K L and Lewis L J 1995 *J. Chem. Phys.* **103** 4632
[4] Ngai K L, Roland C M and Greaves G N 1995 *J. Non-Cryst. Solids* **182** 172
[5] Colmenero J, Arbe A and Alegria A 1993 *Phys. Rev. Lett.* **71** 2603
[6] Colmenero J *et al* 1997 *Phys. Rev. Lett.* **78** 1928
[7] Zorn R *et al* 1995 *Phys. Rev.* E **52** 781
[8] Casalini R, Ngai K L and Roland C M 2003 *Phys. Rev.* B **68** 014201
[9] Schönhals A 2001 *Europhys. Lett.* **56** 815
[10] Novikov V N and Sokolov A P 2003 *Phys. Rev.* E **67** 031507
[11] Stickel F, Fischer E W and Richert R 1996 *J. Chem. Phys.* **104** 2043
[12] Maekawa H, Inagaki Y, Shimokawa S and Yokokawa T 1995 *J. Chem. Phys.* **103** 371
[13] Ngai K L, Bao L R, Lee A F and Soles C L 2001 *Phys. Rev. Lett.* **87** 215901
[14] Adichtchev S V *et al* 2001 *Phys. Rev. Lett.* **87** 055703
[15] Casalini R and Roland C M 2005 *Phys. Rev.* B **71** 014210
[16] Orowan E 1952 *Proc. 1st National Congr. of Applied Mechanics* vol 453 (New York: American Society of Mechanical Engineers)
[17] Goldstein M 1969 *J. Chem. Phys.* **51** 3728
[18] Nemilov S V 2006 *J. Non-Cryst. Solids* **352** 2715
[19] Granato A V and Khonik V A 2004 *Phys. Rev. Lett.* **93** 155502
[20] Dyre J C, Olsen N B and Christensen T 1996 *Phys. Rev.* B **53** 2171
[21] Trachenko K 2007 *Phys. Rev.* B **75** 212201
[22] Trachenko K 2007 *Preprint* cond-mat/0704.2975v1
[23] Yamamuro O, Tsukushi I, Lindqvist A, Takahara S, Ishikawa M and Matsuo T 1998 *J. Phys. Chem.* B **102** 1605
[24] Ngai K L 2007 *J. Non-Cryst. Solids* **353** 709
[25] Ngai K L 2000 *J. Non-Cryst. Solids* **275** 7
[26] Angell C A 1995 *Science* **267** 1924
[27] See supplementary information in Novikov V N and Sokolov A P 2004 *Nature* **431** 961